

AN INTEGRATED VIBRATION-IMAGE PROCEDURE FOR DAMAGE IDENTIFICATION IN STEEL TRUSSES

Marianna Crognale¹, Vincenzo Gattulli¹, Salvador Ivorra² and Francesco Potenza³

¹ DISG, Sapienza University of Rome, Italy
e-mail: {marianna.crognale, [vincenzo.gattulli](mailto:vincenzo.gattulli@uniroma1.it)}@uniroma1.it

² DIC, University of Alicante, Spain
e-mail: sivorra@ua.es

³ INGEO, University of Chieti-Pescara, Italy
e-mail: francesco.potenza@unich.it

Keywords: Damage Identification, Steel Structures, Stochastic Subspace Identification, Fatigue Failure.

Abstract. *The paper deals with structural damage identification in steel trusses. Classical procedure based on dynamic measurements able to detect flexibility changes are complemented with data predicting cracks and their evaluating by image processing. The procedure proposes first a damage index, the Stiffness Reduction Factor (SRF), evaluated on the basis of the error between the predictive truss model and the experimental modal model. Then, a nonlinear FEM model is used to determine fatigue cracks in the truss nodes which are compared with the observed ones determined by image processing. A real case study, the Quisi bridge located in Spain, is used to show the potentiality of the procedure.*

1 INTRODUCTION

Steel truss railway bridges are subject to potential damage, mainly due to fatigue phenomena and corrosion. The monitoring of infrastructures' condition becomes a very important issue to our society for detecting their damage. In last years, vibration-based damage identification methods have been proposed in conjunction with other techniques. Even though the matter has strongly exploited in the scientific community, the raising of innovative technologies in mechatronics, robotics and Information and Communication Technology (ICT) opens up new perspectives in facing the classical problems in the management of infrastructures [9]. Related to this topic, two main research fields could have impact in the inspection and monitoring of infrastructures: automated machine vision-based inspection and the classical structural vibration monitoring. In the first area the use of mobile robots and UAV have strongly increased the acquisition of images to sense the spatial characteristics of the environment, permitting the creation of "cloud" of 3D points. The second area consists in a structural health monitoring system to permit visualization and management of sensor data, data interpretation and analysis and interaction with classical finite element model for structural behavior simulation and model updating. Classical vibration-based monitoring acquires the structural dynamic response, and the corresponding analysis obtains knowledge about the actual mechanical behavior of a structure.

To assess the presence of damage in a steel truss railway bridge, a procedure that links information derived by the vibrations of the bridge with image acquisition by means of long-term monitoring system, has been developed. The paper focuses first on the effects of damage on the static and dynamical response of a nominal model of steel truss. For this purpose, damage is described as a reduction of cross section area of one element of the truss. The direct problem is addressed by FEM and the global modes are identified. The procedure for linear damage detection is tested using pseudo-experimental data, that are generated from the model under white noise. The main modal parameters of the dynamic system are evaluated, before and after damage, using Stochastic Subspace Identification (SSI) method [6-8], based on the assumption that the input is a realization of a stochastic process. The damage identification problem is solved by minimizing an objective function.

A global model of the Quisi Bridge case study is made. The aim of the global analysis is the investigation of the bridge structural behavior to evaluate the structural response due to train crossing. Numerical simulations were conducted before and after damage to study the changes in frequencies and mode shapes due to the presence of damage. In order to perform automatic identification of structural modal parameters based on structural response (output) and to calibrate the numerical global model on experimental data by model updating procedures, an Operational Modal Analysis (OMA) procedure is applied with the purpose of achieve an accurate estimation of natural frequencies. Results obtained from numerical analysis and experimental dynamic tests are mixed together to identify critical details most subjected to fatigue-induced cracks.

In particular, this work aimed at obtaining a better and more accurate comprehension of fatigue phenomena which determine fatigue cracks under the application of a large number of cycles. Thus, a local analysis of critical details is performed to assess the local stress induced by load cycles and the resistance of principal elements.

Preliminary studies performed on the Quisi Bridge, are reported.

2 A PROCEDURE FOR DAMAGE DETECTION IN A TRUSS SYSTEM

In order to assess the presence of damage in a truss structure based on vibration measurements, a sensitivity analysis is performed on a planar truss model (Figure 1) to study the defect-induced reduction of stiffness, (combination of damage intensity and extension).

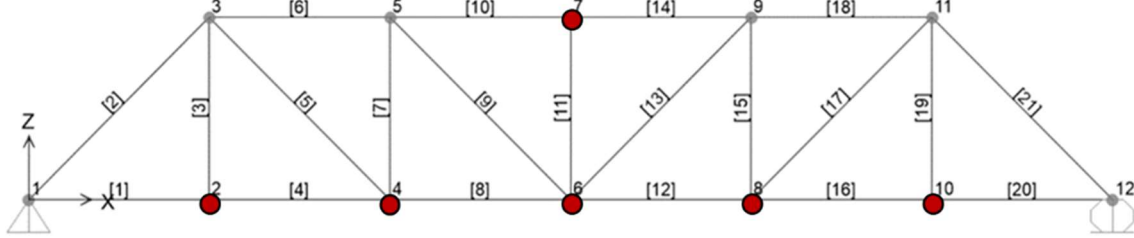


Figure 1: Sketch along with sensor layout in the 2D numerical model.

The damaged truss element is defined and implemented through a classical FEM procedure in which damage is described as a cross-section area reduction and the local stiffness matrix has the following expression:

$$\mathbf{K}_d^e = \frac{EA}{L} \cdot \frac{(1-\zeta)(1+\delta\zeta-\zeta)}{[(1-\zeta)(1-\delta)+\delta]^2} \begin{bmatrix} 1 & 0 & -1 & 0 \\ 0 & 0 & 0 & 0 \\ -1 & 0 & 1 & 0 \\ 0 & 0 & 0 & 0 \end{bmatrix} = \frac{EA}{L} (SRF) \mathbf{K}^e \quad (1)$$

where the damage intensity ζ and extent δ have been represented in non-dimensional form as:

$$\zeta = \frac{EA - EA_d}{EA}, \quad \delta = \frac{L_d}{L}, \quad 0 \leq \zeta \leq 1, \quad 0 \leq \delta \leq 1 \quad (2)$$

SRF is the Stiffness Reduction Factor which is a combination of these two parameters affecting the stiffness and consequently the frequencies [10-11]. Several damage scenarios were considered: the damage parameters were applied consecutively to truss element n. 2, 5 and 6 (Figure 1).

The dependence of the frequencies on the SRF is described by numerical evaluation FEM. The procedure uses pseudo-experimental response, generated from the numerical model under white noise. Vertical accelerations of the bridge were evaluated in several nodes of the model, (indicated in red in Figure 1), and based on these measurements a dynamic identification of the modal parameters was made by SSI in time domain. The inverse problem of damage identification is addressed minimizing an objective function $\mathcal{L}(\zeta, \delta)$ based on frequency measurements, that represents the comparison between the numerical and the experimental dynamical response of the truss. The objective function $\mathcal{L}(\zeta, \delta)$ is defined as follows:

$$\mathcal{L}(\zeta, \delta) = \sum_{i=1}^k \left| \frac{\omega_{d,i}^{EX} - \omega_{d,i}^{NM}(\zeta, \delta)}{\omega_{u,i}^{EX}} \right|^2 \quad (3)$$

Where $\omega_{d,i}^{EX}$ and $\omega_{d,i}^{NM}(\zeta, \delta)$ are the i -th experimental and numerical frequencies of the damaged element respectively, while $\omega_{u,i}^{EX}$ represents the corresponding frequency in the undamaged state. Only an optimum number of modes k are needed to be considered to univocally determine the SRF(δ, ζ) curve in the damage parameter plane (δ, ζ). The number of modes that are necessary to achieve a unique solution in the optimization problem depends on the position of the damaged element in the truss. Figure 2 shows results of the performance of index \mathcal{L} in the detection of curve SRF(δ, ζ) varying the number of modes k . The target point T is indicated with red circle, and the corresponding Γ - curve, in red in Figure 2, is $\Gamma(0.3; 0.5) = 0.76923$.

Table 1 shows the performance of index \mathcal{L} in the detection of the stiffness reduction factor Γ . The number of modes depends on which damaged truss element is considered and on the effects of the vibrational modes. Considering the first three mode of vibration is enough to determine the stiffness reduction factor for this example.

The sensitivity-based strategy can use different type of objective functions and not only frequencies: a modal assurance criterion (MAC and CoMAC); modal flexibility [5] or a combination of the first options [2]. As reported below, a damage identification based on changes in mode shapes is performed for the Quisi Bridge case study.

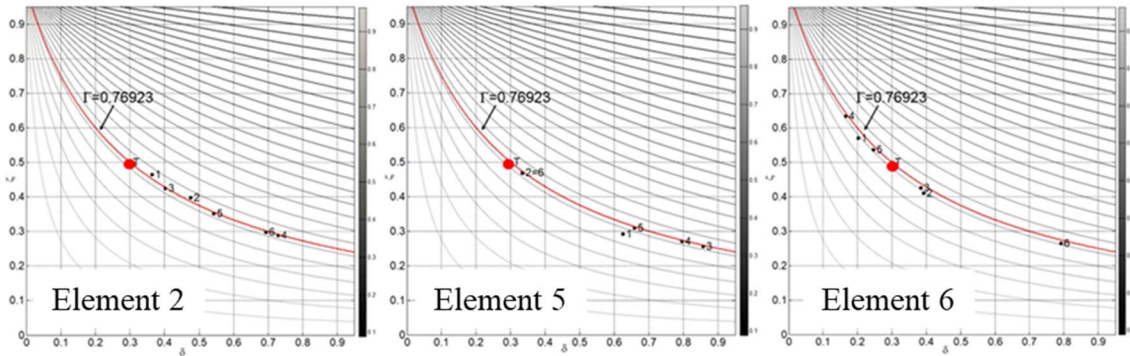


Figure 2: Effects of number of modes in the detection of SRF(δ, ζ) curve respectively in element 2, 5 and 6.

Mode	Element 2		Element 5		Element 6	
	Γ	E_r [%]	Γ	E_r [%]	Γ	E_r [%]
1	0.7596	1.24	0.7958	3.46	0.7879	2.44
2	0.7617	0.90	0.7721	0.39	0.7852	2.08
3	0.7709	0.22	0.7722	0.40	0.7750	0.76
4	0.7714	0.28	0.7725	0.43	0.7766	0.97
5	0.7722	0.39	0.7726	0.44	0.7773	1.05
6	0.7724	0.42	0.7729	0.48	0.7778	1.12

Table 1: Performance of index \mathcal{L} .

3 GLOBAL MODEL: QUISI BRIDGE CASE STUDY

The Quisi Bridge located in Benissa (Alicante) is an historic steel truss railway bridge, which is investigated with different techniques to assess the presence of fatigue damages. It is a XX century steel Bridge and it is part of the 9th FGV Railway Line. The structure consists in a top-bearing Pratt type truss. It is 170 m long with six spans of different length (Figure 3).



Figure 3: Quisi Bridge.

A 3D FE model of the main span permits to evaluate frequencies variation due to damage. Two different damage scenarios (DS) are considered: the first one (DS1) affecting one element of the main span with a stiffness reduction factor of 0.3, the second one (DS2) affecting a group of elements of the truss.

The frequency variation for the first four modes in percentage are reported in the Table 2. The frequency variation produced by damage appears to be quite low evidencing the needs of introducing also other type of damage index based on mode shapes.

The changes of mode shape can be evaluated quantitatively using a well-known correlation measure, the modal assurance criteria (MAC) between two modes shape ϕ_i e ϕ_j , as defined as:

$$MAC_{ij} = \frac{|\phi_i^d \cdot \phi_j^u|^2}{|\phi_i^d|^2 |\phi_j^u|^2} \quad (4)$$

Mode	DS 1	DS 2
	$(f_{iu}-f_{id})/f_{iu}$ [%]	$(f_{iu}-f_{id})/f_{iu}$ [%]
1	0.74	1.91
2	0.54	1.15
3	0.46	1.05
4	0.51	0.56

Table 2: Frequency variations due to the presence of different damage scenario (DS).

Scenario	Mode	UN						
		1	2	3	4	5	6	7
DS1	1	0.984	0.016	0.000	0.000	0.000	0.000	0.000
	2	0.016	0.984	0.000	0.000	0.000	0.000	0.000
	3	0.000	0.000	0.999	0.000	0.000	0.000	0.000
	4	0.000	0.000	0.000	0.999	0.000	0.000	0.000
	5	0.000	0.000	0.000	0.000	0.999	0.000	0.000
	6	0.000	0.000	0.000	0.000	0.000	1.000	0.000
	7	0.000	0.000	0.000	0.000	0.000	0.000	1.000
DS2	1	0.8341	0.1652	0.000	0.000	0.000	0.000	0.000
	2	0.1648	0.8346	0.000	0.000	0.000	0.000	0.000
	3	0.000	0.000	0.9925	0.072	0.000	0.000	0.000
	4	0.000	0.000	0.071	0.9925	0.000	0.000	0.000
	5	0.000	0.000	0.000	0.000	0.9940	0.000	0.000
	6	0.000	0.000	0.000	0.000	0.000	0.8293	0.1679
	7	0.000	0.000	0.000	0.000	0.000	0.1680	0.8317

Table 3: MAC comparing modes from numerical model for damaged and undamaged scenarios. Bold indicates a value calculated with the same mode from the scenario pair.

Table 3 presents MAC values comparing modes obtained by numerical FE model for DS1 and DS2 with the undamaged scenario (UN). The calculated MAC values indicate little change in mode shape for the first damage scenario, with MAC value larger than 0.98 for the first two modes. Marked change in mode shape attributable to the second damage scenario are observed. The most remarkable change occurs in the sixth mode with MAC decreasing to 0.82. A second major change occurs in the first and seventh modes (MAC=0.83). However, in some cases,

MAC fails to reflect the change in mode shape. Another well-known mode shape-derived correlation measure, the coordinate modal assurance criteria (CoMAC), is examined herein. It can be regarded as a point-wise measure of the correlation between two sets of mode shapes and be defined for a measurement point (or degree of freedom) i as:

$$\mathbf{CoMAC}_i = \frac{(\sum_{j=1}^{nm} |\phi_{ij}^d \phi_{ij}^u|)^2}{\sum_{j=1}^{nm} (\phi_{ij}^d)^2 \sum_{j=1}^{nm} (\phi_{ij}^u)^2} \quad (5)$$

The CoMAC between the mode shapes of the damaged and corresponding undamaged scenarios, can be calculated as presented in Figure 4. Although CoMAC is often taken as damage locator for its space information, it might sometimes be affected by its low sensitivity to damage, (as in DS2), and from confusing localization, (as in DS1).

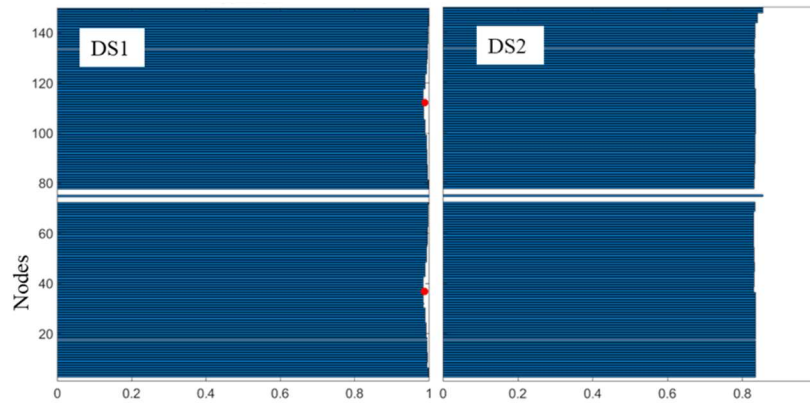


Figure 4: CoMAC comparing modes obtained by numerical model of the main span.

4 EXPERIMENTAL TEST ON THE QUISI BRIDGE

For the Quisi Bridge an experimental dynamic identification of the main features characterizing the dynamic behaviour of the structure, has been performed in order to calibrate the numerical global model on experimental data by updating procedures. Experimental tests constitute a reliable and effective tool for the evaluation of structural dynamic properties. They are composed of experimental acquisitions, obtained recording vibrations of suitable key points of the structure subjected to environmental excitations, and following numerical elaboration of data. Three uniaxial accelerometers were placed on the bridge, one in each mid-span on the right side of the bridge for the first test and on the left side for the second test. Starting from the recorded data, the global modes are identified by Operative Modal Analysis technique (OMA) [4], using the Stochastic Subspace Identification (SSI) in the time domain [1]. Data processing, system identification and modal analysis were performed using MACEC, which is a MATLAB toolbox developed for Experimental and Operational Modal Analysis by the Structural Mechanics division of K.U. Leuven [7].

Figure 5 shows the stabilization diagram and the PSD for the main span of the Quisi bridge in the first OMA test. The identified modal frequencies are reported in Table 4. A total of 4 frequencies for the first test, and 3 frequencies for the second test were identified based on measured response only. In general, a very good accordance is achieved. Due to the low number of accelerometers it is not possible to also identify mode shapes.

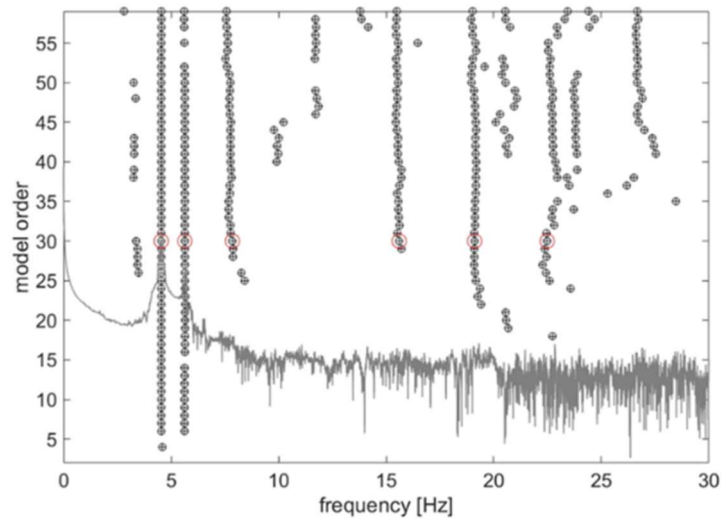


Figure 5: Stabilization diagram and PSD obtained by SSI.

Mode	f_{nm} [Hz]	OMA-test 1		OMA-test 2	
		f_{id} [Hz]	Δ [%]	f_{id} [Hz]	Δ [%]
1	5.05	4.50	10.8	4.50	10.8
2	5.42	5.64	4	5.61	3.5
3	7.30	7.85	7.5	8.42	15
4	15.48	15.60	1	-	-

Table 4: Numerical model frequencies and identified by SSI ones.

5 LOCAL MODEL

The global analysis of the Bridge aimed at the investigation of bridge actual structural performance under train passage, including the assessment of internal forces induced by train into the critical details most subjected to vibration effects. The development of a numerical global model is essential for the identification of the key points that permitting the proper modelling also of critical details. Thus, using forces from the global FE model, it is possible to perform an analysis of the steel connection. There are a lot of benefits of a detailed simulation, first of all the possibility to study system with complex stress distribution, to reproduce correctly local dynamic behaviors, the estimation of action and contact forces, the design of retrofiting for steel connection damaged by corrosion or fatigue cracks. The correct evaluation of local effects generally neglected or simply not consider by standard mechanical modelling is one of the main issues of damage identification. The main effort is the identification of critical details most exposed to damage phenomena, these details can be successful identified by a preliminary analysis of bridge structural behaviour, by means of standard analysis properly refined in order to catch a qualitative indication of local fatigue behaviour.

Once critical details are identified, a nonlinear static analysis can be obtained by means of numerical local models able to represent properly the vibration/distortion phenomena that influence intensity and distribution of stresses. The detailed model using shell FE and links system, is developed by MIDAS-FEA software. The approach to model riveted connection in detailed shell model is made through beam between two surfaces and a system of rigid links between the master node, in the center of the hole, and the slave nodes lying on the circumference of the hole (Figure 6).

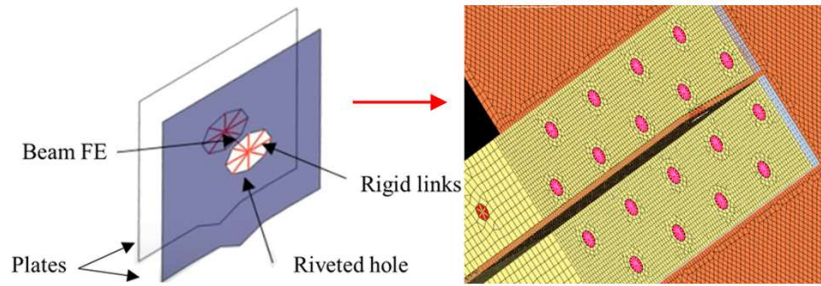


Figure 6: Details of local model.

5.1 Nonlinear static analysis

In this chapter a nonlinear static analysis is carried out. A nonlinear static analysis is a procedure in which the magnitude of the structural loading is incrementally increased in accordance with a certain predefined pattern. With the increase of the magnitude of loading failure mode of the structure are found. Beam element stresses were extracted from the FE global model (Figure 7). For each load step the nonlinear static response of the local model was computed. The stress-strain relation is expressed by an elastic-linear strain hardening law. The elastic-linear strain hardening model supposes that the continuous curve is approximated with two straight lines, the first line has a slope of Young's modulus, while the second straight line presents an idealization for the strain hardening range and has a slope which corresponds to the tangent modulus (E_t), where $E_t < E$. Figure 8 (a-1) shows the distribution of the maximum principal stresses at ten different steps of the incremental static analysis, that are reported in Table 5. The analysis of the figure reveals maximum stress levels in the order of 673 MPa, which represents high values. These maximum stresses are observed on the top of the diagonal member, in the connection plate with the upper chord.

In the Figure 9 (a), the plasticity status obtained by nonlinear static analysis: (a-1) the blue colour indicates the plastic zones that are potential crack locations, (i.e. the connection plate is a plastic region). Figure 9 (a-2) shows a detail of the double strap joint with two rows of rivets in the plate: from a static point of view both rows carry the same load which implies the same stress on the rivets, but from a fatigue point of view the two rows are in a different position, the holes in row B of the plate are loaded by P_B only and in row A the same load P_A is present on the holes but the load already introduced in row B is also passing these holes. The latter load is called a bypass load. Nevertheless, for this case study the holes in row A are more severely loaded than holes in row B and thus will be more fatigue critical. Fatigue cracks will occur in the row A cause of plastic deformation around the holes under static load. In the Figure 9 (b), the flux of the principal stresses is highlighted by blue colour (compression) and red colour (tension) lines with lengths proportional to the stress intensity.

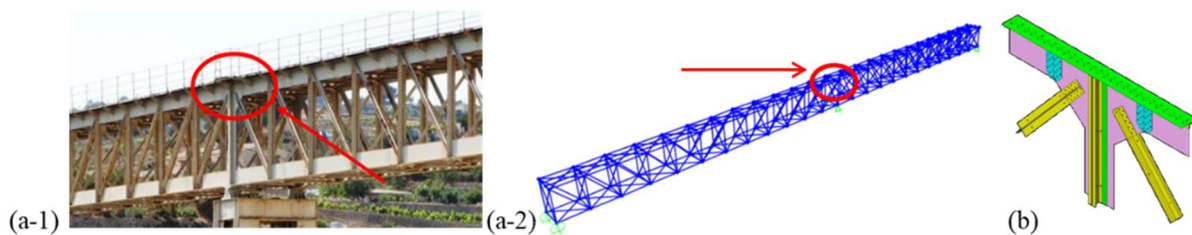


Figure 7: (a-1) Actual photo of the critical point of the Quisi Bridge where fatigue phenomena could arise; (a-2) Location of the potential fatigue critical node; (b) FE local model by MIDAS-FEA.

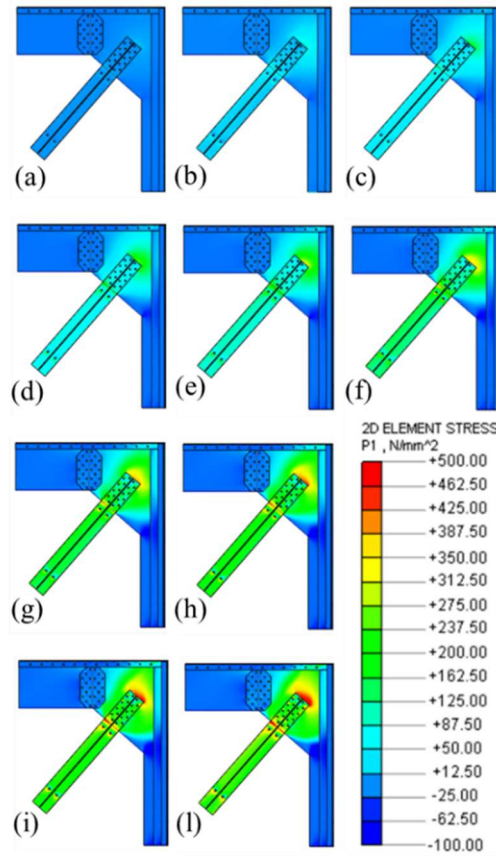


Figure 8: (a-l) Maximum principal stresses obtained by static nonlinear numerical analysis.

Step	T [kN]	σ_1 [MPa]
(a)	385	70.21
(b)	770	134.82
(c)	1155	203.13
(d)	1540	270.95
(e)	1925	338.39
(f)	2310	405.26
(g)	2695	472.58
(h)	3080	539.87
(i)	3465	607.17
(l)	3850	673.03

Table 5: Load steps applied and the corresponding maximum principal stress levels, for a finite element of the model located in the upper side of the diagonal member.

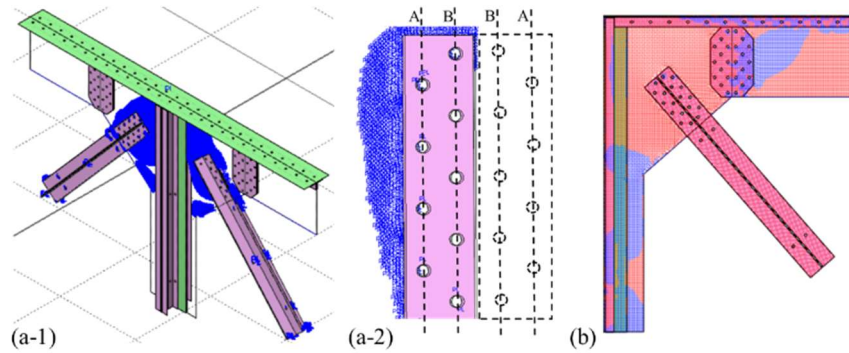


Figure 9: Results obtained by static NL numerical analysis: (a) plasticity element status of the joint: (a-1) the blue colour indicates the plastic zones, (a-2) detail of the double strap joint with two rows of rivets at both side of the joint; (b) flux of the principal stresses: blue colour indicates compression and red colour indicates tension.

5.2 Fatigue analysis

Fatigue failure is defined as the tendency of a material to fracture by means of progressive brittle cracking under repeated alternating or cyclic stresses of an intensity considerably below the normal strength. Although the fracture is of a brittle type, it may take some time to propagate, depending on both the intensity and frequency of the stress cycles. All structures and mechanical components that are cyclically loaded can fail by fatigue. Fatigue failure in structures frequently occurs in joints. Understanding the fatigue mechanism is essential to considering various technical conditions which affect fatigue life and fatigue crack growth. Fundamental requirements during design and manufacturing to avoid fatigue failure are different for each different case and should be considered during the design phase. Fracture specifically describe the growth or propagation of a crack once it has been initiated and has given rise to many so-called crack growth methodologies. Fatigue analysis can be performed based on stress (stress-life method) and strain (strain-life method).

The stress-life method is mainly used for fatigue analysis under the condition of a low stress level relative to the yield stress. The stress-life method predicts the extent of fatigue under a given loading history using the relationship between the number of loading cycles (N) and stress amplitude (S) at the time when failure occurs from a cyclically applied constant load. The S-N curve shows the relationship between the stress amplitude (S) occurring from a cyclic loading of constant amplitude applied to the structure and the number of cycles to failure (N) when the stress of the corresponding amplitude is repeated. For a fatigue analysis using the stress-life method, a linear elastic analysis on the structure is performed first, and then equivalent stresses (such as principal stresses) are obtained. These stresses are then applied to an S-N curve to predict the number of loading cycles required to reach the fatigue failure in conjunction with detail category tables, to obtain a good estimation of the safety level of each detail on the bridge. In Eurocode 3 [3], 14 S-N curves, which are equally spaced in log scale, as shown in Figure 10 (a), are defined. Each curve is characterized by the detail category $\Delta\sigma_C$. The slope coefficient m is equal to 3 for stress range above the constant amplitude fatigue limit (CAFL), $\Delta\sigma_D$, at 5 million cycles, and equal to 5 for stress range between the CAFL and the cut-off limit, $\Delta\sigma_L$, at 10 million cycles.

For riveted connections, Italian railways company imposed a value of 71 MPa, corresponding to the detail category 71, see Figure 11 (b), where the nominal stress $\Delta\sigma$ has to be calculated on the net cross-section (gross cross-section minus section of rivet holes in the critical section).

According to Eurocode 3 part 1-9, the fatigue strength value $\Delta\sigma_C$ is divided by γ_{MF} , so obtaining $\Delta\sigma_D = \Delta\sigma_C / \gamma_{MF} = 71/1.35 \text{ MPa} = 52 \text{ MPa}$. The fatigue strength curve is defined as follows:

$$(\Delta\sigma_R)^m N_R = (\Delta\sigma_C)^m 2 \cdot 10^6, \quad m = 3 \text{ for } N \leq 5 \cdot 10^6 \quad (6)$$

$$(\Delta\sigma_R)^m N_R = (\Delta\sigma_C)^m 2 \cdot 10^6, \quad m = 5 \text{ for } 5 \cdot 10^6 \leq N \leq 1 \cdot 10^8 \quad (7)$$

$$\Delta\sigma_L = (5/100)^{1/5} \Delta\sigma_D, \quad (\text{cut-off limit}) \quad (8)$$

When several stress amplitudes exist, the degree of damage of a material is calculated by accumulating individual damages from each of the stress amplitudes. Using the number of cycles corresponding to a specific stress amplitude, n_i , and fatigue life, N_i , the cumulative damage is calculated using Equation (9). The fatigue life of a structure is the reciprocal of the damage according to Equation (10).

$$\text{Damage} = \sum_i \frac{n_i}{N_i} \quad (9)$$

$$\text{Fatigue Life} = \frac{1}{\text{Damage}} \quad (10)$$

The riveted single-track railway Bridge was built in 1917 and was in use until a few years ago. After over 90 years of service, there is a motivation for assessment since the bridge has reached the end of its design working life. Therefore, an assessment is carried out to determine the residual service life of the bridge. Since the bridge has been in use for 94 years, there is a higher probability of failure due to fatigue than due to static overloading.

Data on traffic was collected from the railway's archives. A single type of locomotive has transited this line, (Locomotive series 1000), as sketched in Figure 11.

Results of fatigue analysis performed using MIDAS-FEA are reported in Figures 12 and 13. From the second fatigue result, it is noticed that there is no remaining fatigue life for elements in blue colour, it had expired 4 years before the year in which this assessment was undertaken. The member chosen for the analysis cannot be considered safe anymore. It should be noted that each specific structural element has a different fatigue life.

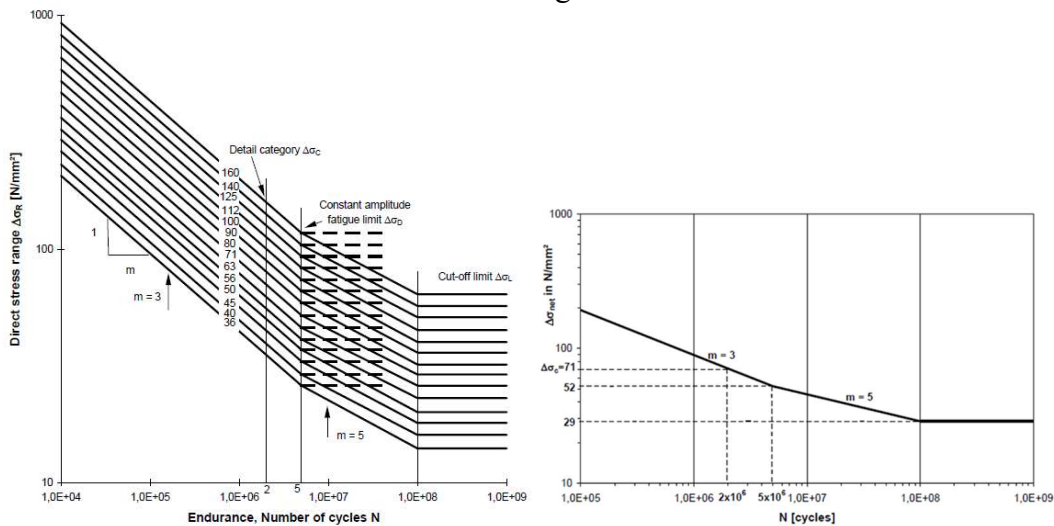


Figure 10: (a) Fatigue strength curves for nominal stress ranges for structural steel components; (b) S/N curve for the fatigue assessment of old riveted steel bridges.

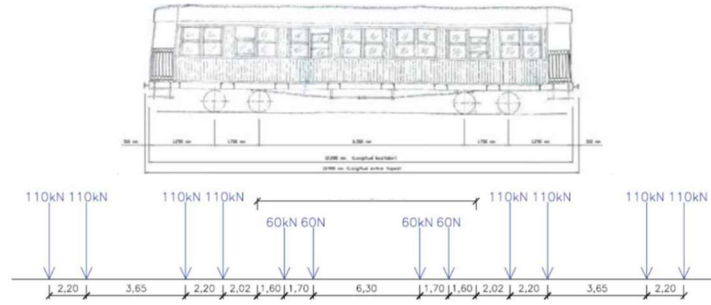


Figure 11: Sketch of Locomotive series 1000 and distance between axles and axle loads.

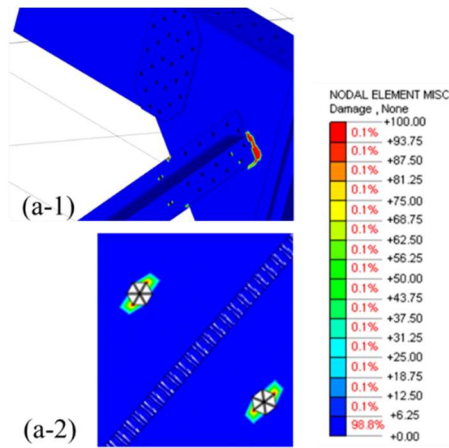


Figure 12: Fatigue analysis results in terms of damage: (a-1) - (a-2) detail views of damage contour.

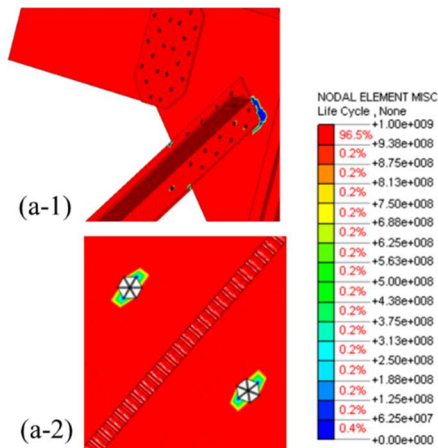


Figure 13: Fatigue analysis results in terms of fatigue life: (a-1) fatigue life of the joint; (a-2) detail of the holes in the diagonal element.

6 LONG-TERM MONITORING

An image acquisition by means of long-term monitoring system on the Quisi Bridge, permits on one hand to improve the procedure and, on the other hand, to obtain the description of current fatigue cracks on the bridge. On-site inspections were carried out by means of non-destructive testing of the connections of the bridge. Gamma radiation radiographs, (gammagraphy), were performed. The tests were performed by the TÜV SÜD ATISAE Laboratory and the test

standard procedure UNI EN ISO 5579 was used. The gammagraphy was carried out in a total of 160 connection geometry of the viaduct. The existence of cracks, cavities, inclusions, fusion and penetration defects, imperfections in shape and dimensions and other types of imperfections have been analyzed. In general, the state of the connections is very acceptable. However, small fissures have been identified in four zones of the bridge, shown in Figure 14, 15 and 16. It is worth noting that the first crack on the first isostatic span (Figure 14) and also the second crack on the iperstatic span (Figure 15) are located down the rivet cap or in the interior of the plate inside the union of several steel sheets. Through visual inspection it is not possible to detect these cracks. The third crack, (Figure 16 (b)), could be an original failure dating back to the stage of fabrication process of the rivet on the bridge; the fourth crack (Figure 16 (c)) is of the same type as the first two. On the isostatic spans the cracks are in a similar position this could be due to the loop effect generated by the train passage. No crack was observed in the position subjected to local modeling. Thus, a second detailed local model is under realization.

The image processing of the crack images has been carried out through segmentation by thresholding. Segmentation in a digital processing is a process of partitioning an image into significant regions and it is used to extract objects from the image. As in Figure 17 the first step is the thresholding that from a grayscale image returns a binary image, subsequently the noise removal, in the third step the assessment of the boundaries of the identified regions, the regions associated with the crack are the regions 3 and 4, and these will be therefore measurable (parameter estimation of the crack). The same procedure is in progress for other crack images, it is requiring pre-processing to highlight the crack from the background (Figure 18). Based on the information extracted from the images acquisition and the newer local model behavior, it will be possible to update the global model considering the presence of fatigue crack.

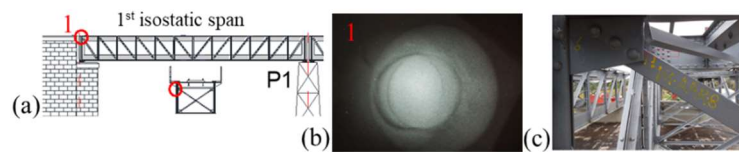


Figure 14: (a) Bridge critical point where crack 1 is observed; (b) Gammagraphy of a crack identified; (c) Cross view where the crack 1 is observed.

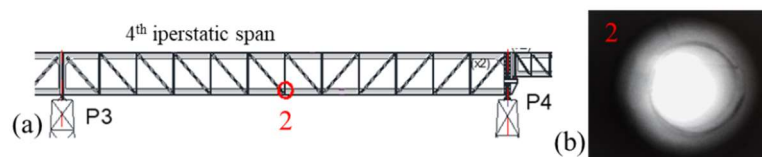


Figure 15: (a) Bridge critical point where crack 2 is observed; (b) Gammagraphy of a crack identified.

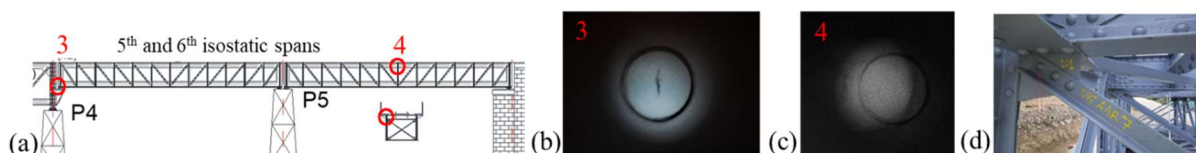


Figure 16: (a) Bridge critical point where cracks 3 and 4 are observed; (b) - (c) Gammagraphies of the two cracks identified; (d) Cross view where the crack 4 is observed.

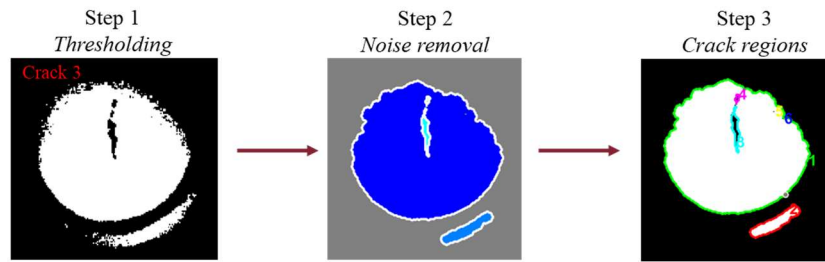


Figure 17: The architecture of image processing-based crack detection for crack 3.

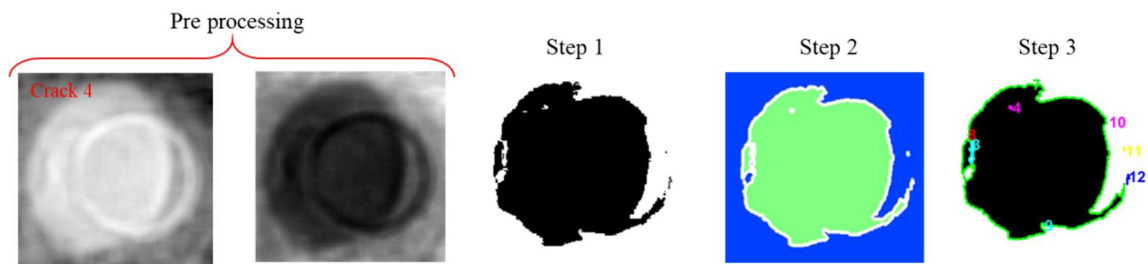


Figure 18: Image preprocessing for crack 4.

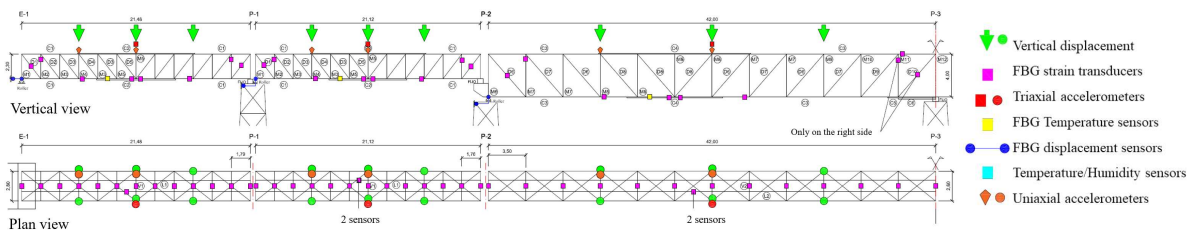


Figure 19: Layout of the permanent monitoring system and types of sensors.

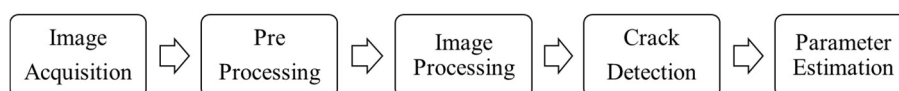


Figure 20: The architecture of image processing-based crack detection.

7 CONCLUSIONS

A procedure to identify damage in a steel truss bridge has been proposed. The results obtained through pseudo-dynamic testing and FEM analysis for a simple truss evidences the obtainable resolutions in damage indicator with the increase of a number of modes. For the main span of the Quisi Bridge the damage changes, affected both one single element and then a group of elements, do not affect to the main frequencies of the bridge so, a mode shape based method is performed. Natural frequency changes alone may not be sufficient for a unique identification of the location of structural damage.

From the results of stress intensity obtained in the global model, the critical point is selected to analyze the fatigue phenomena in the local model.

Fatigue damage appears in the form of fatigue cracks and can occur in primary loaded or secondary elements. Since fatigue failure is depending on the load spectra over the service life, consequently, existing steel structures suffer more from fatigue and accumulate more damage the older the bridges are.

Fatigue crack initiation in structural details is generally expected where stress concentrations may occur, such as holes as showed by the presented detailed FEM model of a joint of the Quisi Bridge. These results are comparable with the crack identified by Gammagraphy. More data are expected for the Quisi Bridge in which a permanent monitoring system will be install even with image acquisition. Figure 19 shows the experimental setup with an important number of channels, the data acquisition is done under environmental condition.

Concerning the image-based detection of fatigue cracks, the general architecture of the method is shown in Figure 20 and it includes: an initially collect the image of the structure which will be subjected to the crack detection process (image acquisition), the pre-processing of the images with segmentation, the crack detection using the result of the processed image and finally the crack feature extraction that is the step in which the detected cracks are separated based on the width, depth, area or length of the crack.

The available data will permit to perform a nonlinear model updating through an error criterion based on crack pattern and frequency and modal shape variations.

ACKNOWLEDGMENTS

This paper is a part of a project that has received funding from the Research Fund for Coal and Steel under grant agreement No 800687. (DESDEMONA EU project)

REFERENCES

- [1] B. Peeters, G. De Roeck, Reference-based stochastic subspace identification for output-only modal analysis, *Mechanical Systems and Signal Processing*, 1999.
- [2] D.J. Ewins, *Modal Testing: Theory and Practice*, New York, John M. Wiley & Sons, 2000.
- [3] EN 1993-1-9, *Eurocode 3: Design of steel structures – Part 1-9: Fatigue*, 2004.
- [4] L. Zhang, T. Wang, Y Tamura, A Frequency-Spatial Decomposition (FSDD) Technique for Operational Modal analysis. *IOMAC 2005 Procedia: 1st International Operational Modal Analysis Conference*, April 26-27, Copenhagen, Denmark, 2005.
- [5] Y. Gao, B. F. Spencer Jr., D. Bernal, Experimental Verification of the Flexibility-Based Damage Locating Vector Method, *Journal of Engineering Mechanics*, 2007.
- [6] A. Deraemaeker, E. Reynders, G. De Roeck, J. Kullaa, Vibration-based structural health monitoring using output-only measurements under changing environment. *Mechanical Systems and Signal Processing*, 22, 34-56, 2008.
- [7] E. Reynders, M. Schevenels, G. De Roeck, MACEC: A Matlab toolbox for experimental and operational analysis, *Report BWM-2008-07*, April 2008.
- [8] D. Foti, V. Gattulli, F. Potenza, Output-Only Identification and Model Updating by Dynamic Testing in Unfavourable Conditions of a Seismically Damaged Building. *Computer-Aided Civil and Infrastructure Engineering*, vol. 29(9), pp 659-675, 2014, doi: 10.1111/mice.12071.

- [9] F. Potenza, G. Castelli, V. Gattulli, E. Ottaviano, Integrated process of image and acceleration measurements for damage detection, EUROODYN 2017.
- [10] M. Crognale, V. Gattulli, S. Ivorra, F. Potenza, Dynamics and damage sensitivity of the Quisi steel truss bridge. Gattulli Vincenzo, Oreste Bursi, and Daniele Zonta, eds. *ANCRiSST 2019 Procedia: 14th International Workshop on Advanced Smart Materials and Smart Structures Technology. Vol. 45*. Sapienza Università Editrice, Agosto 2019.
- [11] M. Crognale, V. Gattulli, A. Paolone, F. Potenza, A procedure for damage identification in a steel truss. XXIV Congresso AIMETA 2019, Associazione Italiana di Meccanica Teorica e Applicata 15-19 Settembre 2019.